Panchromatic Ru(II)-polypyridyl complexes as NIR emitters

Amlan K. Pal,*[,a] Venkata Nanda Kishor Babu Adusumalli [b]

[a] Organic Semiconductor Centre, School of Chemistry, University of St Andrews, St Andrews, Fife, U.K., KY16 9ST

[b] Department of Chemical Sciences and Centre for Advanced Functional Materials, Indian Institute of Science Education and Research (IISER) Kolkata, Mohanpur, India

Supporting Information

Materials, methods and instrumentation

Nuclear magnetic resonance (NMR) spectra were recorded in CD_3CN at room temperature (r.t.) on a Bruker AV400 (400 MHz) spectrometer for ^1H NMR, at 100 or 125 MHz for ^{13}C NMR, respectively, as mentioned in the experimental section. The following abbreviations have been used for multiplicity assignments: "s" for singlet, "d" for doublet, "t" for triplet, "m" for multiplet, and "br" for broad. Chemical shifts are reported in parts per million (ppm) relative to respective residual solvent protons. Chromatography was performed on columns with an i.d. of 25-30 mm on silica gel (Silicagel 60, 40-63 μm). The progress of the catalytic photoredox reactions and the elution of the products were followed by TLC (silica gel on plastic sheets, 250 μm with indicator F-254). Compounds were visualized under UV light.

Accurate mass measurements were performed on a LTQ Orbitrap XL1 mass spectrometer in positive nanospray mode. Appropriate $[M-n(PF_6)]^{n+}$ species were used for empirical formula determination, and exact masses were calculated using Analyst® QS Software from Applied Biosystems by EPSRC National Mass Spectrometry Service Centre, Swansea University. Elemental analyses of complexes **1** and **2** were performed by Mr. Stephen Boyer, London Metropolitan University. All photophysical measurements were carried out in deaerated acetonitrile at r.t. in septa-sealed quartz cells. Absorption spectra were measured on a Cary 500i UV-Vis-NIR Spectrophotometer. The sample solutions for the emission spectra were prepared in HPLC grade MeCN and degassed by three freeze-pump-thaw N_2/vacuum cycles. Steady state emission and time-resolved emission spectra were recorded at 298 K using a Shimadzu RF-6000 and an Edinburgh Instruments F980, respectively. Samples for steady state measurements were excited at 550 nm or 500 nm, as mentioned in the footnote of **Table S11**, while samples for time-

resolved measurements were excited at 378 nm using a PDL 800-D pulsed diode laser. The emission profiles were checked at different excitations at 460, 500, 650 nm, except at 550 nm and the emissions of these complexes were found to be centred at ~ 835 nm in all cases. Emission quantum yields were determined using the optical dilution method.[1] A stock solution with absorbance of *ca.* 1 was prepared and then four dilutions were prepared to obtain solutions with absorbances of *ca.* 0.1 0.075, 0.05 and 0.025, respectively. The Beer-Lambert law was found to be linear at the concentrations of the solutions. The steady state emission spectra (λ_{exc} = 500 nm) were then measured after the solutions were degassed by three freeze-pump-thaw N_2/vacuum cycles per sample prior to spectrum acquisition. For each sample, linearity between absorption and emission intensity was verified through linear regression analysis and additional measurements were acquired until the Pearson regression factor (R^2) for the linear fit of the data set surpassed 0.9. Individual relative quantum yield values were calculated for each solution and the values reported represent the slope value. The equation $\Phi_s = \Phi_r(A_r/A_s)(I_s/I_r)(n_s/n_r)^2$ was used to calculate the relative quantum yield of each of the sample, where Φ_r is the absolute quantum yield of the reference, *n* is the refractive index of the solvent, *A* is the absorbance at the excitation wavelength, and *I* is the integrated area under the corrected emission curve. The subscripts s and r refer to the sample and reference, respectively. Acetonitrile solution of $[Ru(bpy)_3]Cl_2$ (bpy = 2,2′-bipyridine) (Φ_r = 9.5%) was used as the external reference.[2] Electrochemical measurements were carried out in argon-purged purified acetonitrile at room temperature with a BAS CV50W multipurpose equipment interfaced to a PC. The working electrode was a glassy carbon electrode. The counter electrode was a Pt wire, and the pseudo-reference electrode was a silver wire. The reference was set using an internal 1 mM ferrocene/ferrocinium sample at 380 mV *vs.* SCE in acetonitrile. The concentration of the compounds was about 1 mM. Tetrabutylammonium hexafluorophosphate

(TBAP) was used as supporting electrolyte and its concentration was 0.10 M. Cyclic voltammograms of **1** and **2** were obtained at a scan rate of 100 mVs^{-1}. The criteria for reversibility were the separation of 60 mV between cathodic and anodic peaks, the close to unity ratio of the intensities of the cathodic and anodic currents, and the constancy of the peak potential on changing scan rate. Differential pulse voltammetry was conducted with a sweep rate of 20 mVs^{-1} and a pulse amplitude, width and period of 50 mV, 50 ms and 200 ms, respectively.

Experimental uncertainties are as follows: absorption maxima, ±2 nm; molar absorption coefficient, 10%; redox potentials, ± 10 mV, emission maxima, ±2 nm, quantum yield, ±5%.

1,3,4,6,7,8-Hexahydro-2*H*-pyrimido[1,2-*a*]pyrimidine (**H-hpp**), 2,6-dibromopyridine, 2,6-dichloropyrazine, (±)BINAP, BuOK^t, ammonium hexafluorophosphate, potassium nitrate were purchased from Aldrich and used as received. 2-Acetylpyridine, n-butanol and 4-formylbenzoic acid were purchased from Fluorochem and used as received. Pd(OAc)$_2$, hydrated RuCl$_3$ were purchased from Pressure Chemicals. Ligands **L1** (or dgpy),[3] **L2** (or dgpz)[4] and CO$_2$HPh-tpy (CO$_2$HPh-tpy = 4-([2,2':6',2"-terpyridin]-4'-yl)benzoic acid)[5] were synthesized following literature procedures.

[Ru(**L1**)(CO$_2$HPh-tpy)][(PF$_6$)$_2$] (**1**):
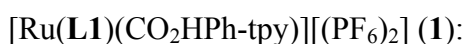
A mixture of [Ru(CO$_2$HPh-tpy)Cl$_3$] (100 mg, 0.178 mmol), **L1** (76 mg, 0.214 mmol, 1.2 equiv.) in nitrogen-degassed *n*-butanol was heated to reflux for 20 h to give a red-brown solution. After cooling of the mixture to ambient temperature, the solution was filtered under vacuum and the filtrate was evaporated to dryness. To the resulting purple solid was added an aliquot of (20 mL) saturated aqueous NH$_4$PF$_6$ solution and the mixture was sonicated for 5 minutes with stirring. The purple solid was filtered, washed with water (2 x 30 mL) and then dried under vacuum. The

crude product was purified by silica column chromatography using 7:1 (v/v) CH_3CN: aqu. saturated KNO_3 as the eluant. The second purple band was collected, solvent was evaporated to dryness and the nitrate anion was again metathesized with hexafluorophosphate by addition of an aliquot of saturated aqu. NH_4PF_6. The product was obtained as a purple solid after filtration and drying under vacuum. Crystals suitable for X-ray crystallography of **1** could be grown by diffusing diethyl ether into a concentrated acetonitrile-acetone solution of the title compound. Yield = 115 mg (59%). $\mathbf{R_f}$: 0.45 in 7:1 (v/v) CH_3CN:satd. aqu. KNO_3. **¹H NMR (400 MHz, acetonitrile-d_3)**: δ/ppm = 8.73 (s, 2H), 8.57 (d, J = 8.1 Hz, 2H), 8.29 (d, J = 8.4 Hz, 2H), 8.15 (dd, J = 9.3, 8.3 Hz, 3H), 8.05 (d, J = 5.5 Hz, 2H), 8.00 (td, J = 7.8, 1.5 Hz, 2H), 7.51 – 7.44 (m, 4H), 4.05 (s, 2H), 3.20 (s, 6H), 2.36 (m, 8H), 1.66 (s, 2H), 1.46 (s, 2H), 1.19 (s, 2H), 0.87 (s, 2H). **¹³C NMR (100 MHz, acetonitrile-d_3)**: δ/ppm = 167.23, 159.72, 158.96, 155.90, 154.07, 154.03, 142.70, 142.04, 140.98, 137.25, 131.65, 131.51, 128.37, 126.97, 124.02, 121.08, 112.91, 49.63, 48.82, 48.46, 43.89, 23.39, 23.13. **HRMS (ESI)**, m/z: 404.1252 $[M-2PF_6]^{2+}$ ($C_{41}H_{42}N_{10}O_2Ru$ requires 404.1265), 953.2140 $[M-PF_6]^+$ ($C_{41}H_{42}N_{10}O_2RuPF_6$ requires 953.2177). **Anal. Calc.** for $C_{41}H_{42}N_{10}O_2RuP_2F_{12}$: C, 44.86; H, 3.86; N, 12.76. Found: C, 45.02; H, 3.86; N, 12.74.

[Ru(**L2**)(CO_2HPh-tpy)][$(PF_6)_2$] (**2**):
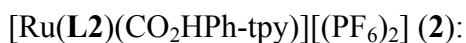
A mixture of [Ru(CO_2HPh-tpy)Cl_3] (100 mg, 0.178 mmol), **L2** (76 mg, 0.214 mmol, 1.2 equiv.) in nitrogen-degassed *n*-butanol was heated to reflux for 20 h to give a red-brown solution. After cooling of the mixture to ambient temperature, the solution was filtered under vacuum and the filtrate was evaporated to dryness. To the resulting purple solid was added an aliquot of (20 mL) saturated aqueous NH_4PF_6 solution and the mixture was sonicated for 5 minutes with stirring. The purple solid was filtered, washed with water (2 x 30 mL) and then dried under vacuum. The crude product was purified by silica column chromatography using 7:1 (v/v) CH_3CN: aqu.

saturated KNO_3 as the eluant. The second purple band was collected, solvent was evaporated to dryness and the nitrate anion was again metathesized with hexafluorophosphate by addition of an aliquot of saturated aqu. NH_4PF_6. The product was obtained as a purple solid after filtration and drying under vacuum. Yield = 99 mg (51%). **R_f**: 0.40 in 7:1 (v/v) CH_3CN:satd. aqu. KNO_3. **^1H NMR (400 MHz, acetonitrile-d_3)**: δ/ppm = 8.75 (s, 2H), 8.59 (d, J = 17.0 Hz, 4H), 8.29 (d, J = 8.3 Hz, 2H), 8.15 – 8.10 (m, 4H), 8.06 – 7.99 (m, 2H), 7.48 (ddd, J = 7.4, 5.7, 1.3 Hz, 2H), 4.15 (br, s, 2H), 3.19 (m, 6H), 2.36 (m, 8H), 1.60 (d, J = 44.3 Hz, 6H), 0.91 (s, 2H). **^{13}C NMR (100 MHz, acetonitrile-d_3)**: δ/ppm = 159.53, 158.27, 154.06, 153.61, 151.26, 149.91, 148.06, 146.32, 144.32, 137.71, 133.15, 131.27, 127.99, 127.09, 124.31, 121.16, 49.45, 48.94, 48.47, 47.38, 23.48, 23.02. **HRMS (ESI)**, m/z: 404.6238 [M-2PF$_6$]$^{2+}$ ($C_{40}H_{41}N_{11}O_2Ru$ requires 404.6244), 954.2114 [M-PF$_6$]$^+$ ($C_{40}H_{41}N_{11}O_2RuPF_6$ requires 954.2130). **Anal. Calc.** for $C_{40}H_{41}N_{11}O_2RuP_2F_{12}$: C, 43.72; H, 3.76; N, 14.02. Found: C, 43.61; H, 3.74; N, 13.76.

Figure S1. ^1H NMR spectrum of **1** in CD_3CN at 400 MHz at room temperature.
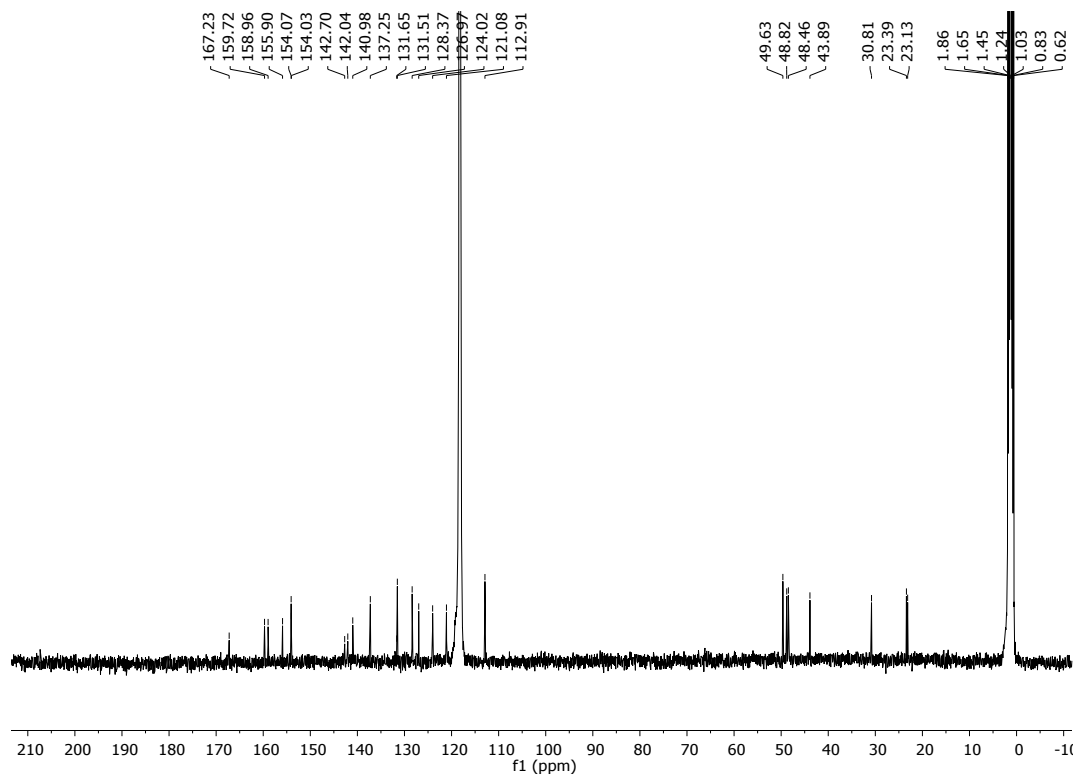
Figure S2. ^{13}C NMR spectrum of **1** in CD$_3$CN at 100 MHz at room temperature.
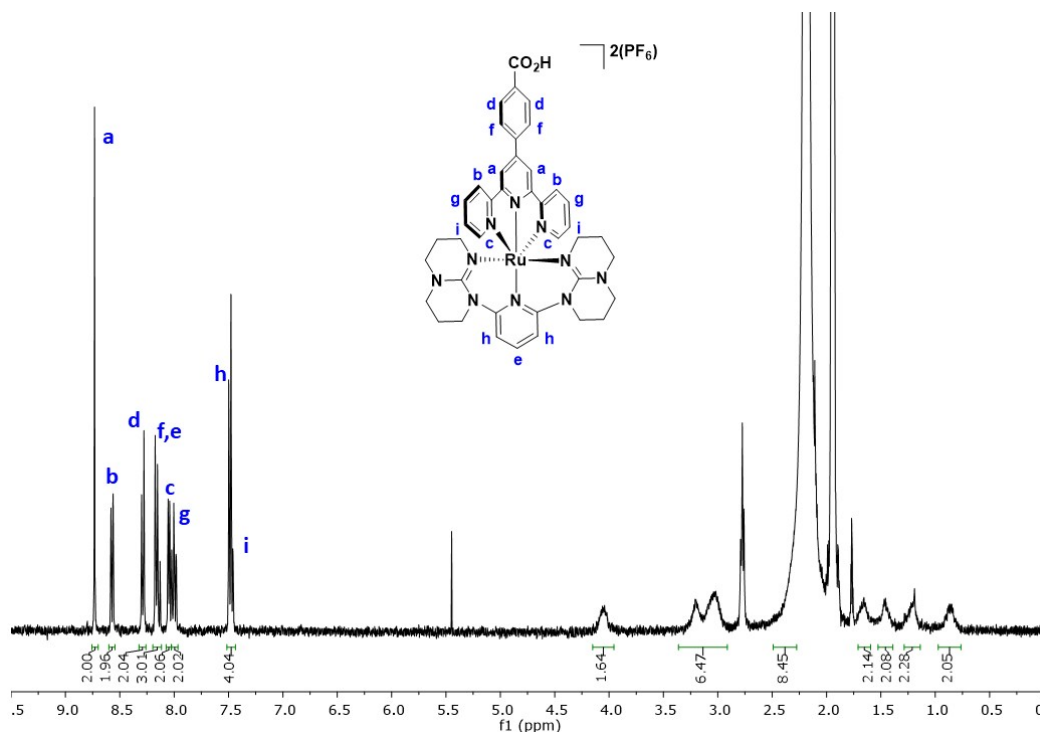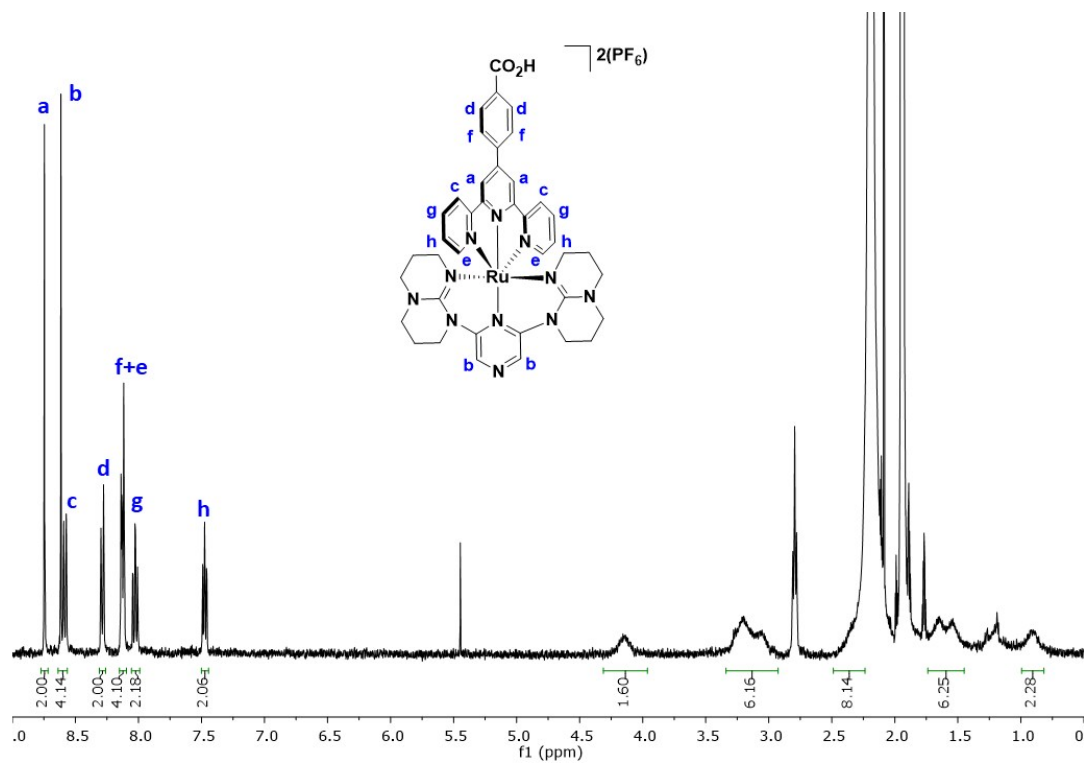

Figure S3. ^{1}H NMR spectrum of **2** in CD$_3$CN at 400 MHz at room temperature.
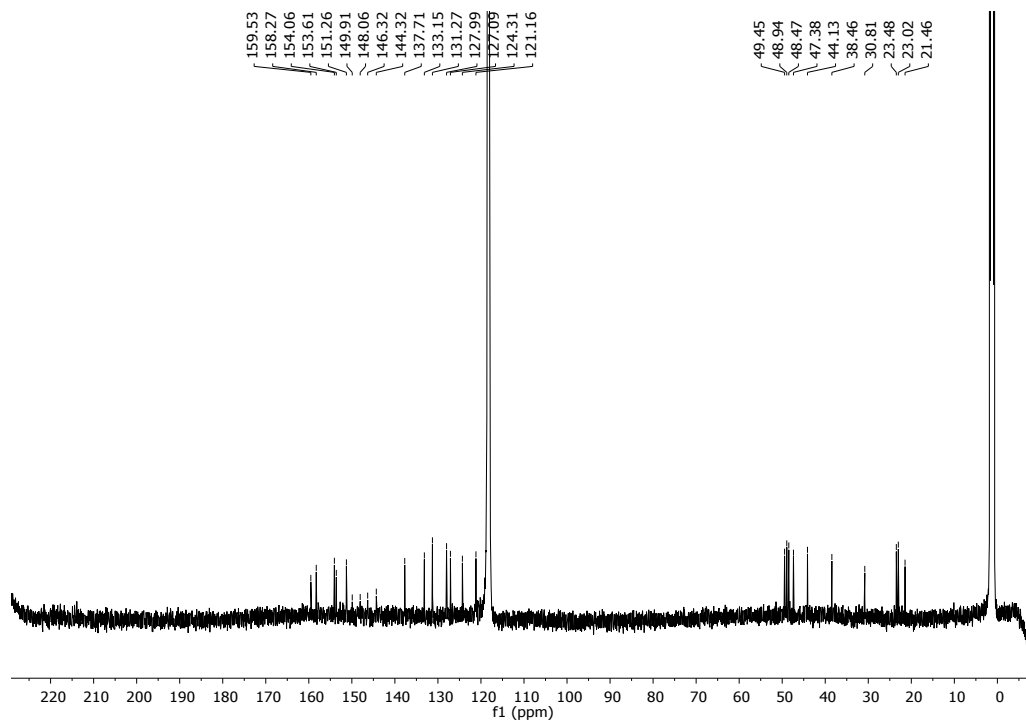
Figure S4. ^{13}C NMR spectrum of **2** in CD$_3$CN at 125 MHz at room temperature.
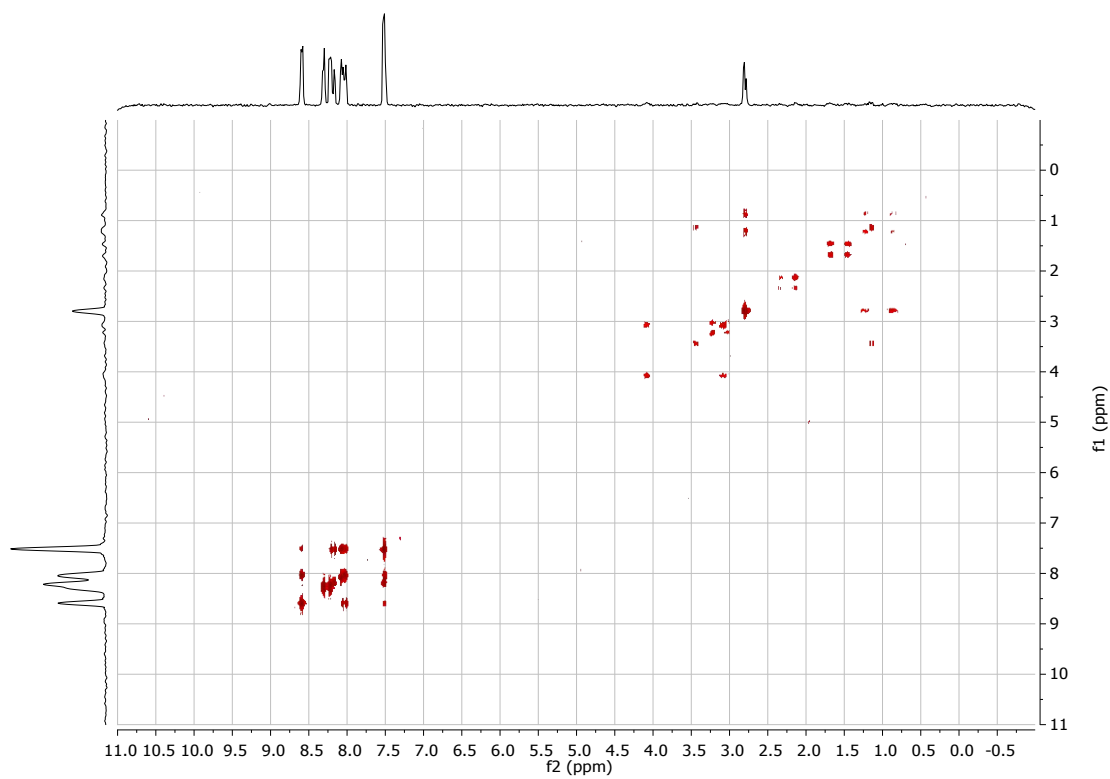
Figure S5. ^{1}H-^{1}H COSY NMR spectrum of **1** in CD$_3$CN at 400 MHz at room temperature.
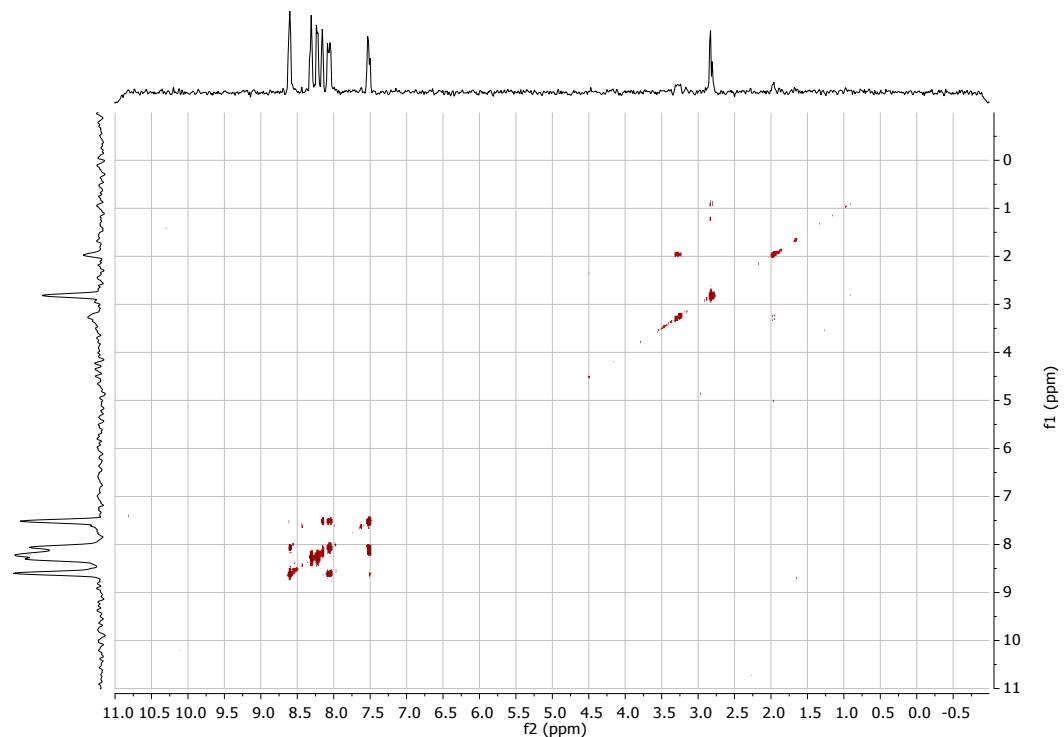
Figure S6. ^{1}H-^{1}H COSY NMR spectrum of **1** in CD$_3$CN at 400 MHz at room temperature.
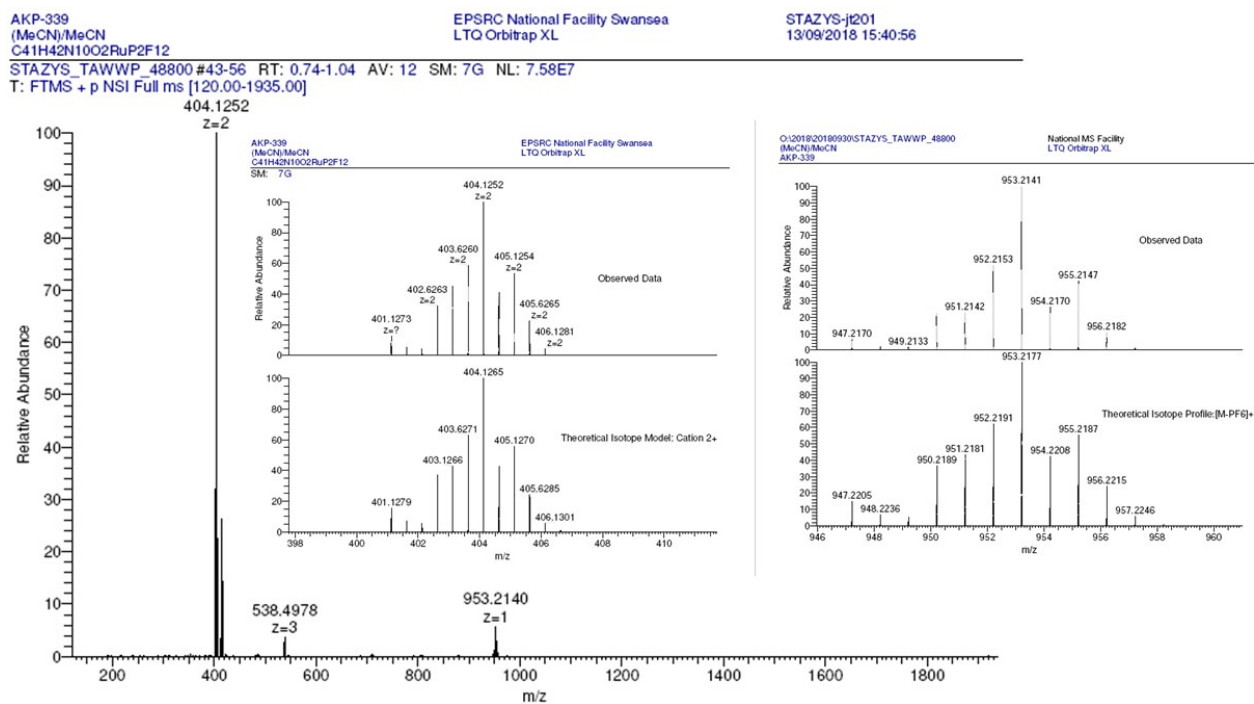
Figure S7. High resolution NSI mass spectrum of **2** in CH$_3$CN (insets show the overlay of experimental and theoretical isotropic distribution patters of $[M-2PF_6]^{2+}$ (left) and $[M-PF_6]^{+}$ (right)).
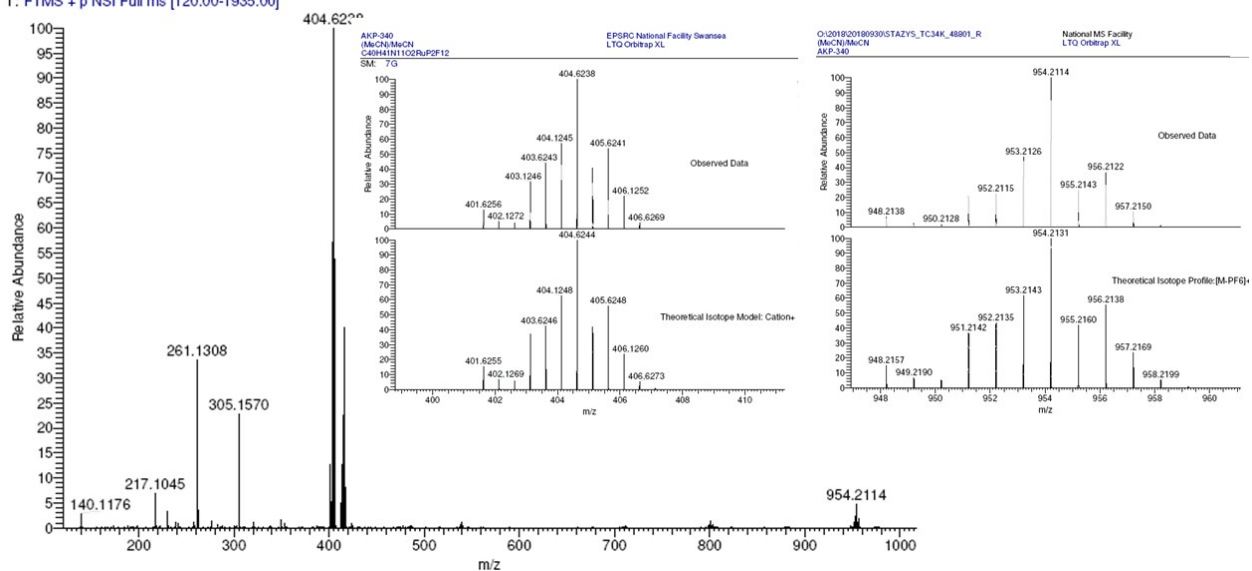
Figure S8. High resolution NSI mass spectrum of **2** in CH$_3$CN (insets show the overlay of experimental and theoretical isotropic distribution patters of [M-2PF$_6$]$^{2+}$ (left) and [M-PF$_6$]$^{+}$ (right)).

X-ray diffraction studies:

X-ray crystallographic data were collected from a single crystal sample, which was mounted on a loop fiber. Data were collected using a Bruker diffractometer equipped with a Bruker APEX-II CCD detector, a Kappa goniometer and a Cu-K$_\alpha$ source (λ = 1.54178 Å) at 100(2) K. The crystal-to-detector distance was 4.0 cm, and the data collection was carried out in 1024 x 1024 pixel mode. The initial unit cell parameters were determined by a least-squares fit of the angular setting of strong reflections, collected by a 110.0 degree scan in 110 frames over three different parts of the reciprocal space.

The diffraction quality of the crystals were checked, revealing in some cases poor diffraction with a large amount of diffuse scattering, signaling extensive crystal disorder. Data collection, cell refinement and data reduction were done using APEX2[6] and SAINT.[7] Absorption corrections were applied using SADABS.[8] Structures were solved by direct methods using SHELXS2012 and refined on F^2 by full-matrix least squares using SHELXL2012.[9] All non-hydrogen atoms were refined anisotropically. Hydrogen atoms were refined isotropic on calculated positions using a riding model. For complex **1**, atom C36 in the hpp moiety was found to be disordered over two positions. This minor positional disorder was not taken into account for modelling. The P atom and some fluorine atoms in the PF$_6$ anions of the structure of **1** were also found to be positionally disordered. For complex **1** the highest difference peak is in close proximity to the atom C36, which was found to exhibit positional disorder. In addition, in **1** four more peaks with density around 1 e/Å^3 were present essentially due to the positional disorder of the hexafluorophosphate anion in the crystal employed, which was the best available.
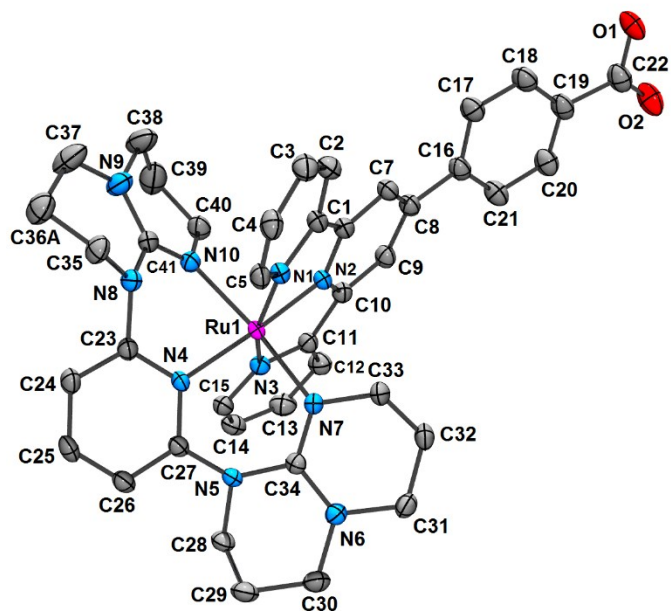
Figure S9. ORTEP view of complex **1**. Hydrogen atoms, solvated acetone molecule and anions are not shown for clarity. Ellipsoids correspond to a 50% probability level.

Table S1. Crystallographic data for complexes **1**.

Compound	1
CCDC	1843763
Formula	$[C_{41}H_{42}N_{10}O_2Ru][2(PF_6)]\cdot C_3H_6O$
Mw (g/mol); $d_{calcd.}$ (g/cm^3)	1153.91; 1.6714
T (K); F(000)	100(2); 1177.66
Crystal System	Triclinic
Space Group	P-1
Unit Cell:	
a (Å)	8.4554(2)
b (Å)	13.7942(4)
c (Å)	20.8461(5)
α (°)	97.2010(14)
β (°)	94.2490(15)
γ (°)	106.8770(14)
V (Å^3); Z	2292.64(10); 2
θ range (°); completeness	2.15-71.58; 0.9721
R_{fle}:collec./indep.; R_{int}	47548/8587; 0.0250
μ (mm^{-1})	4.35
R1(F); wR(F^2); GoF(F^2)^a	0.0399; 0.1040; 1.036
Residual electron density	1.83; -1.03

^{a}R1(F) based on observed reflections with I>2σ(I) for **1**; wR(F^2) and GoF(F^2) based on all data for all compounds.

Table S2. Comparison of bond distances and angles in **1**.

Compound		Bond Length			Angle		
1		Obs. (X-ray)	Calc. (DFT)		Obs. (X-ray)	Calc. (DFT)
	Ru1-N1	2.066(3)	2.15071	N1-Ru1-N3	159.07(10)	156.162
	Ru1-N2	1.939(2)	2.00868	N7-Ru1-N10	172.40(10)	171.160
	Ru1-N3	2.087(3)	2.15135	N1-Ru1-N2	80.02(10)	78.048
	Ru1-N4	2.070(2)	2.12726	N2-Ru1-N3	79.06(10)	78.115
	Ru1-N7	2.059(3)	2.15135	N4-Ru1-N17	85.98(10)	85.244
	Ru1-N10	2.089(3)	2.15622	N4-Ru1-N10	86.74(10)	85.954

Table S3. Electrochemical data for **L1**, **L2**, **1** and **2**.

Compound	$E_{1/2}(ox)^a$ / V		$E_{1/2}(red)^a$ / V			$\Delta E_{1/2}$ / V
L1(dgpy)[b]	1.11 (308)	0.77 (irr)[c]	----			----
L2(dgpz)[b]	1.14 (189)	0.77 (irr)[c]	-1.99 (irr)[c]			2.76
1	0.52 (66)		-1.49 (61)	-2.03 (72)	-2.73 (irr)[c]	2.33
2	0.59 (59)		-1.44 (66)	-1.89 (101)	-2.17 (190)	2.37

[a]Potentials are in volts *vs*. SCE for acetonitrile solutions, 0.1 M in [*n*-Bu$_4$N]PF$_6$, recorded at 25 ± 1 °C at a sweep rate of 100 mVs^{-1} for cyclic voltammetry and 20 mVs^{-1} for differential pulsed voltammetry. The difference between cathodic and anodic peak potentials (mV) is given in parentheses. [b]From ref 4. [c]Irreversible; oxidation potential is given for anodic wave, while reduction potential is given for cathodic wave.
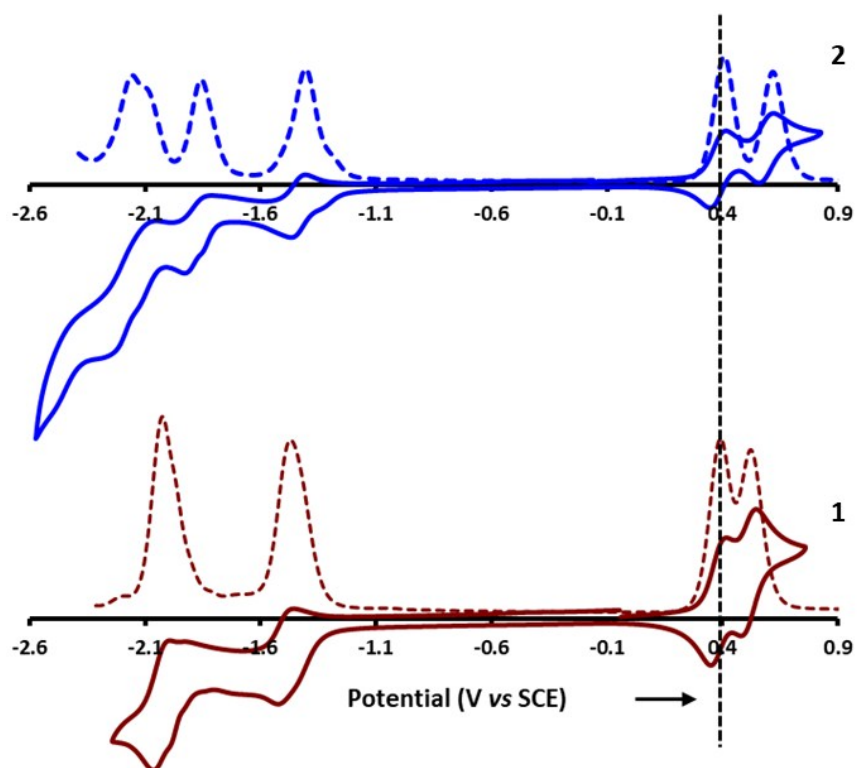
Figure S10. Cyclic voltammograms of **1** (maroon) and **2** (blue) in bold lines in dry, degassed CH$_3$CN. Differential pulse voltammograms of **1** (maroon) and **2** (blue) are presented in dotted lines. Vertical line at 0.38 mV represents the Fc$^+$/Fc couple in both the voltammograms.
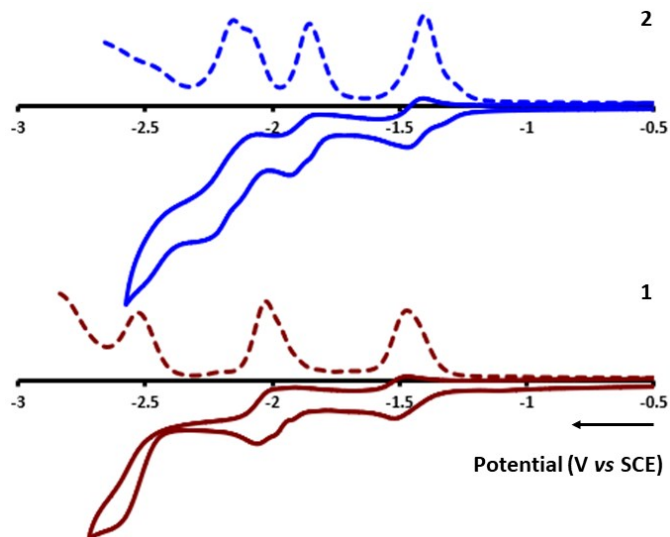
Figure S11. Cyclic voltammograms of **1** (maroon) and **2** (blue) in bold lines in dry, degassed CH_3CN in the negative potential only. Differential pulse voltammograms of **1** (maroon) and **2** (blue) are presented in dotted lines.

DFT Calculations:

All calculations were performed with the Gaussian09[10] suite of programs employing the DFT method, the Becke three-parameter hybrid functional,[11] and Lee-Yang-Parr's gradient-corrected correlation functional (B3LYP).[12] Singlet ground state geometry optimizations for $[\mathbf{1}]^{2+}$ and $[\mathbf{2}]^{2+}$ were carried out at the (R)B3LYP level in the gas phase, using their respective crystallographic structures as starting points. All elements except cobalt were assigned the 6-31G(d,p) basis set.[13] The double-ζ quality SBKJC-VDZ basis set[14] with an effective core potential and one additional f-type polarization was employed for the Ru(II)-ion. Vertical electronic excitations based on (R)B3LYP-optimized geometries were computed for $[\mathbf{1}]^{2+}$ and $[\mathbf{2}]^{2+}$ using the TD-DFT formalism[15a,b] in acetonitrile using conductor-like polarizable continuum model (CPCM).[16a-c] Vibrational frequency calculations were performed to ensure that the optimized geometries represent the local minima and there are only positive eigenvalues. The electronic distribution and localization of the singlet excited states were visualized using the electron density

16

difference maps (ED-DMs).[17] *Gausssum 2.2* and *Chemissian* were employed to visualize the absorption spectra (simulated with Gaussian distribution with a full-width at half maximum (fwhm) set to 3000 cm^{-1}) and to calculate the fractional contributions of various groups to each molecular orbital. All calculated structures and Kohn-Sham orbitals were visualized with ChemCraft.[18]

Table S4. M.O. Composition of [**1**]$^{2+}$ in Singlet ($S = 0$) Ground State (b3lyp/SBKJC-VDZ[Ru]6-31G**[C,H,N,O]).

MO	Energy (eV)	Composition			
		Ru	CO$_2$HPh-tpy	Py	hpp
LUMO+4	-5.84	5	90	1	4
LUMO+3	-5.91	2	95	0	3
LUMO+2	-6.06	3	4	81	12
LUMO+1	-6.81	2	97	0	1
LUMO	**-6.98**	**7**	**87**	**1**	**5**
HOMO	**-9.89**	**49**	**20**	**4**	**27**
HOMO-1	-9.93	54	10	1	35
HOMO-2	-10.4	72	18	8	2
HOMO-3	-10.77	0	100	0	0
HOMO-4	-10.89	3	82	1	14

Table S5. M.O. Composition of [**2**]$^{2+}$ in Singlet ($S = 0$) Ground State (b3lyp/SBKJC-VDZ[Ru]6-31G**[C,H,N,O]).

MO	Energy (eV)	Composition			
		Ru	CO$_2$HPh-tpy	Pz	hpp
LUMO+4	-5.97	5	90	1	4
LUMO+3	-6.03	2	95	0	3
LUMO+2	-6.62	4	5	79	12
LUMO+1	-6.94	2	97	0	1
LUMO	**-7.13**	**7**	**85**	**3**	**5**
HOMO	**-10.09**	**50**	**18**	**3**	**29**
HOMO-1	-10.1	51	11	2	36
HOMO-2	-10.61	70	20	8	2
HOMO-3	-10.84	0	100	0	0
HOMO-4	-11	5	81	1	13

Table S6. UV-vis absorption data of **L1**, **L2**, **1**, **2** and benchmark complex [Ru(tpy)$_2$]$^{2+}$.[a]

Compound	λ_{max}, nm (ε x 10^3, M^{-1}cm^{-1})
L1 (dgpy)	228 (29.0), 311 (12.8)
L1 (dgpz)	224 (26.9), 340 (14.1)
1	226 (40.7), 246 (37.3), 282 (40.7), 289 (44.2), 317 (23.6), 395 (10.9), 541 (9.5), 620 (6.1)
2	224 (37.5), 245 (31.8), 279 (31.8), 288 (36.6), 320 (26.7), 396 (9.5), 538 (8.8), 612 (6.9)
[Ru(tpy)$_2$]$^{2+}$[b]	474 (10.4)

[a]data in dry acetonitrile at room temperature. [b]from 19.

Table S7. Selected Transitions from TD-DFT calculations of [**1**]$^{2+}$ in the Singlet Ground State (b3lyp/SBKJC-VDZ[Ru]6-31G**[C,H,N,O], CPCM (CH$_3$CN)).

state	λ/nm	λ/nm (ε x 10^3 M^{-1}cm^{-1}) [expt.]	f	Major transition(s)	character
91	226	226 (40.7)	0.1451	H-4->L+9 (62%), H-2->L+12 (12%)	CO$_2$HPh-tpy(π) to CO$_2$HPh-tpy(π*)
65	249	246 (37.3)	0.2396	H-5->L+4 (16%), H-3->L+6 (52%)	CO$_2$HPh-tpy(π) to Py(π*) (major) + CO$_2$HPh-tpy(π) to CO$_2$HPh-tpy(π*) (minor)
40	284	282 (40.7)	0.1712	H-7->L+1 (32%), H-3->L+3 (54%)	CO$_2$HPh-tpy(π) to CO$_2$HPh-tpy(π*) (major) + hpp(π) to CO$_2$HPh-tpy(π*) (minor)
37	290	289 (44.2)	0.2547	H-9->L (72%), H-6->L+1 (18%)	CO$_2$HPh-tpy(π) to CO$_2$HPh-tpy(π*) (major) + hpp(π) to CO$_2$HPh-tpy(π*) (minor)
30	317	317 (23.6)	0.3792	H-6->L (57%), H-4->L+1 (12%), H-2->L+5 (16%)	hpp(π) to CO$_2$HPh-tpy(π*) (major) + CO$_2$HPh-tpy(π) to CO$_2$HPh-tpy(π*) (minor) + Ru(dπ) to Py(π*) (minor)
8	398	395 (10.9)	0.1719	H-1->L+2 (56%), H->L+2 (31%)	Ru(dπ) to Py(π*)
5	497	541 (9.5)	0.2276	H-2->L (23%),	Ru(dπ) to CO$_2$HPh-

state	λ/nm	λ/nm (ε x 10^3 $M^{-1}cm^{-1}$) [expt.]	f	Major transition(s)	character
				H-1->L (20%), H->L+1 (40%)	tpy(π*) (major) + hpp(π) to CO$_2$HPh-tpy(π*) (minor)
1	638	620 (6.1)	0.0167	H-1->L (15%), H->L (81%)	Ru(dπ) to CO$_2$HPh-tpy(π*) (major) + hpp(π) to CO$_2$HPh-tpy(π*) (minor)

Table S8. Selected Transitions from TD-DFT calculations of [**2**]$^{2+}$ in the Singlet Ground State (b3lyp/SBKJC-VDZ[Ru]6-31G**[C,H,N,O], CPCM (CH$_3$CN)).

state	λ/nm	λ/nm (ε x 10^3 $M^{-1}cm^{-1}$) [expt.]	f	Major transition(s)	character
90	231	224 (37.5)	0.1671	H-9->L+6 (44%), H-7->L+6 (17%), H-3->L+8 (11%)	CO$_2$HPh-tpy(π) to Pz(π*) (major) + hpp(π) to Pz(π*) (minor) + CO$_2$HPh-tpy(π) to CO$_2$HPh-tpy(π*) (minor)
73	245	245 (31.8)	0.1557	H-5->L+5 (64%)	CO$_2$HPh-tpy(π) to hpp(π*)
48	271	279 (31.8)	0.1255	H-4->L+3 (65%), H-1->L+9 (23%)	CO$_2$HPh-tpy(π) to hpp(π*) (major) + hpp(π) to hpp(π*) (minor)
40	287	288 (36.6)	0.2605	H-9->L (26%), H-6->L+1 (62%)	CO$_2$HPh-tpy(π) to CO$_2$HPh-tpy(π*) (major) + hpp(π) to CO$_2$HPh-tpy(π*) (minor) + Pz(π) to CO$_2$HPh-tpy(π) (minor)
30	317	320 (26.7)	0.3387	H-6->L (43%), H-4->L+1 (20%), H-2->L+4 (20%)	CO$_2$HPh-tpy(π) to CO$_2$HPh-tpy(π*) (major) + hpp(π) to CO$_2$HPh-tpy(π*) (minor) + Pz(π) to CO$_2$HPh-tpy(π) (minor) + Ru(dπ) to CO$_2$HPh-tpy(π*) (minor)
10	389	396 (9.5)	0.191	H-2->L+2 (76%), H-1->L+3 (10%)	Ru(dπ) to Pz(π*) (major) + Ru(dπ) to CO$_2$HPh-tpy(π*) (minor)

2	562	538 (8.8)	0.1248	H-1->L (78%), H->L+1 (11%)	Ru(dπ) to CO$_2$HPh-tpy(π*) (major) + hpp(π) to CO$_2$HPh-tpy(π*) (minor)
1	622	612 (6.9)	0.0169	H->L (96%)	Ru(dπ) to CO$_2$HPh-tpy(π*) (major) + hpp(π) to CO$_2$HPh-tpy(π*) (minor)
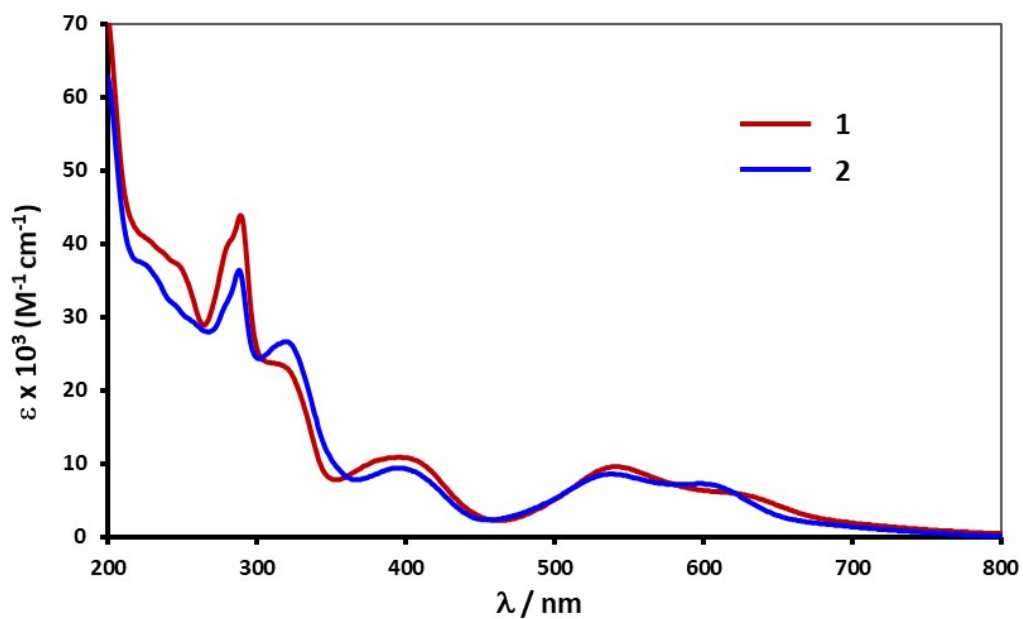
Figure S12. UV-vis absorption spectra of **1** and **2** in dry MeCN at r.t.
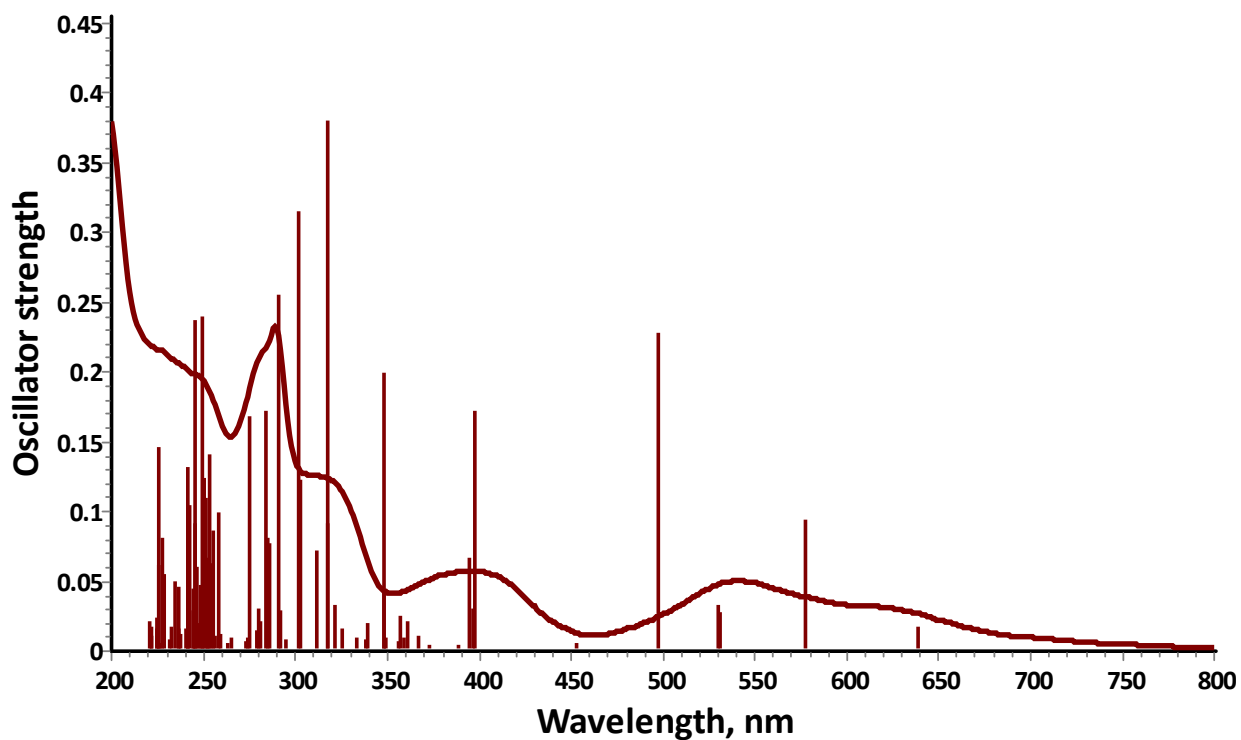
Figure S13. Overlay of experimental (curved line) absorption spectra and TD-DFT calculated oscillator strengths (red bars) at different wavelengths of **1**, at ambient temperature in dry acetonitrile.
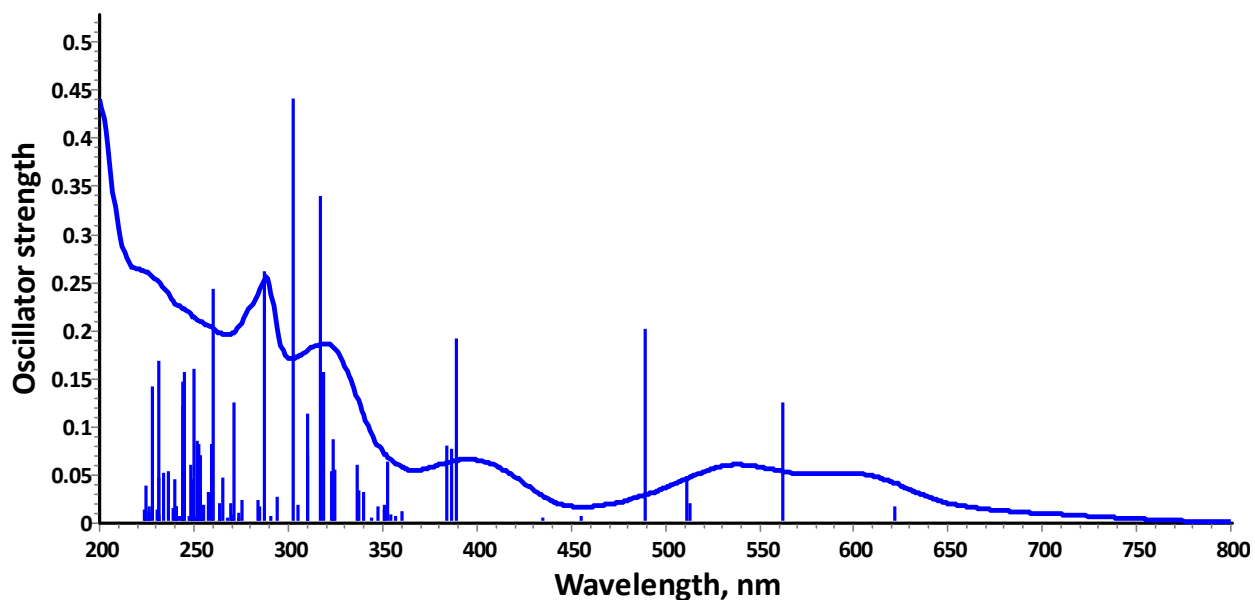
Figure S14. Overlay of experimental (curved line) absorption spectra and TD-DFT calculated oscillator strengths (red bars) at different wavelengths of **2**, at ambient temperature in dry acetonitrile.

Table S9. Relevant photophysical data of complexes **1** and **2** in dry, degassed MeCN solution at 298 K.

Cmpd	298 K[a]				
	λ_{em} (nm)[b]	Φ_{PL} (%)[c]	τ_{PL} (ns) [χ^2][d]	k_r^e (x 10^5 s^{-1})	k_{nr}^f (x 10^7 s^{-1})
1	839	0.5	9.03 (100%) [1.06]	5.53	11.02
2	834	0.6	11.06 (100%) [1.04]	5.44	8.99

[a]In dry, degassed MeCN solution; [b]λ_{exc} = 550 nm, [c]Using [Ru(bpy)$_3$]Cl$_2$ in MeCN (Φ_{PL} = 9.5%, λ_{exc} = 500 nm); [d]λ_{exc} = 378 nm (χ^2 denotes the fitting value), [e]calculated using $K_r = \Phi_{PL} / \tau_{PL}$, [f]calculated using $K_{nr} = (1 - \Phi_{PL}) / \tau_{PL}$.
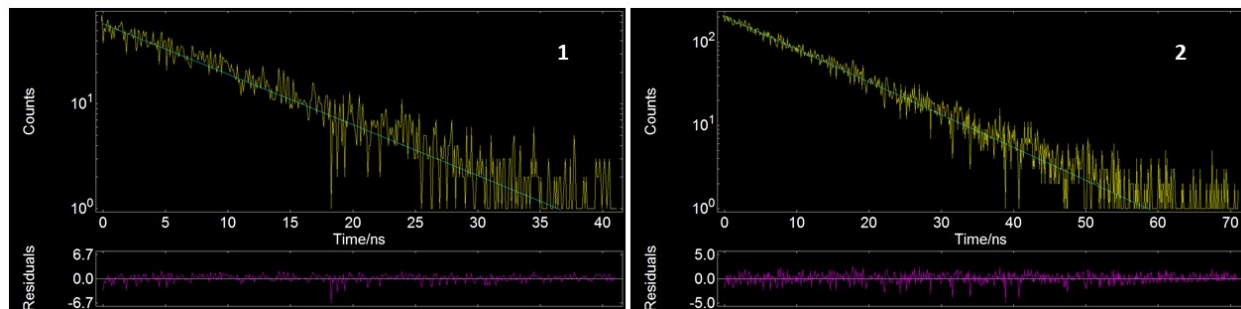
Figure S15. Photoluminescence decay profiles of complexes **1** and **2** at r.t. in dry, degassed acetonitrile (λ_{exc} = 378 nm).

[**1**]$^{2+}$ [**2**]$^{2+}$
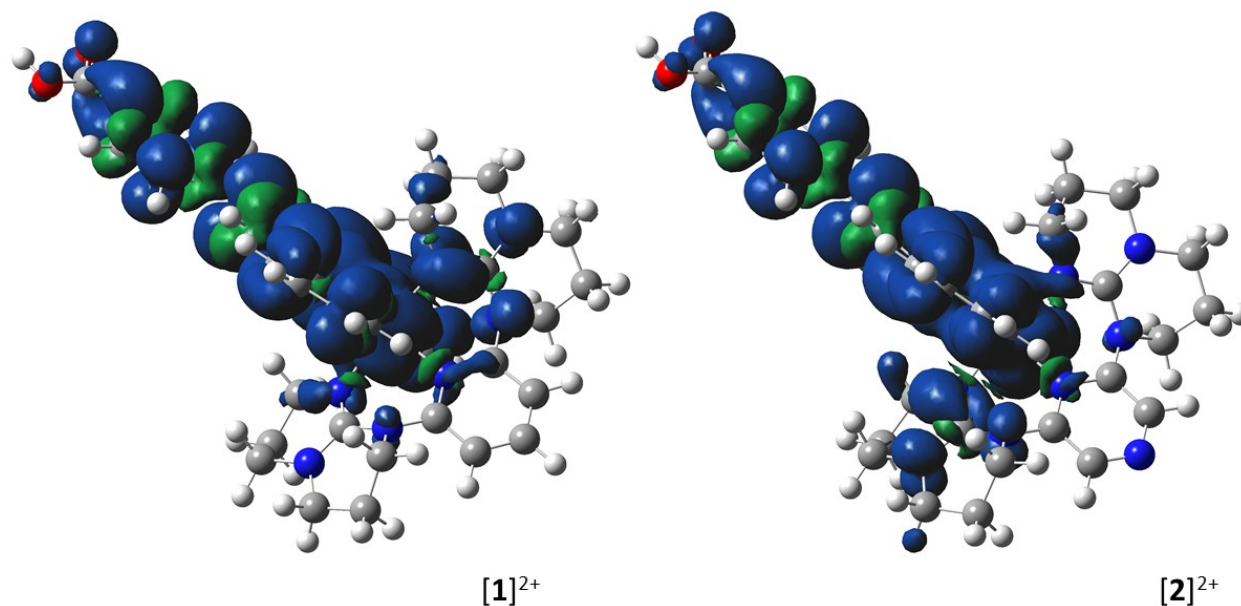
Figure S16. Triplet spin density profiles of [**1**]$^{2+}$ and [**2**]$^{2+}$ using unrestricted DFT calculations ((rb3lyp/SBKJC-VDZ[Ru]6-31G**[C,H,N,O], CPCM (CH$_3$CN)).

Table S10. Optimized Atomic coordinates obtained from DFT calculations of [**1**]$^{2+}$

Center Number	Atomic Number	Atomic Type	Coordinates (Angstroms)		
			X	Y	Z
1	44	0	1.110083	0.015884	-0.022054
2	8	0	-10.040741	1.094281	-0.324353
3	1	0	-10.999488	0.965961	-0.272335
4	8	0	-10.088703	-1.023168	0.458673
5	7	0	0.665062	0.996370	-1.887269
6	7	0	-0.902061	0.013510	-0.030006
7	7	0	0.656523	-0.989311	1.832201
8	7	0	3.244626	-0.007290	0.015977
9	7	0	3.219124	-2.394063	0.158153
10	7	0	2.176640	-4.040800	-1.156257
11	7	0	1.287544	-1.853323	-1.079115
12	7	0	3.224200	2.380263	-0.152111
13	7	0	2.128468	4.097537	1.011162
14	7	0	1.248656	1.901466	1.020630
15	6	0	-0.678488	1.134361	-2.113918
16	6	0	-1.154391	1.705819	-3.298497
17	1	0	-2.219303	1.813432	-3.463439
18	6	0	-0.256234	2.129581	-4.273655
19	1	0	-0.618546	2.562046	-5.200062
20	6	0	1.109943	1.969119	-4.043629
21	1	0	1.847068	2.273245	-4.777924
22	6	0	1.522341	1.403455	-2.840728
23	1	0	2.572606	1.259685	-2.619370
24	6	0	-1.566582	0.590601	-1.062447
25	6	0	-2.961145	0.594057	-1.088156
26	1	0	-3.496897	1.024710	-1.924910
27	6	0	-3.689970	-0.005349	-0.045253
28	6	0	-2.963100	-0.610138	0.996771
29	1	0	-3.503510	-1.062068	1.819151
30	6	0	-1.569779	-0.590721	0.985206
31	6	0	-0.688379	-1.155945	2.030442
32	6	0	-1.174436	-1.790359	3.178181
33	1	0	-2.240244	-1.918043	3.321919
34	6	0	-0.284941	-2.250138	4.145605
35	1	0	-0.654526	-2.738277	5.040817
36	6	0	1.081512	-2.054822	3.948339
37	1	0	1.811520	-2.381228	4.680363
38	6	0	1.504249	-1.423369	2.782088
39	1	0	2.554940	-1.243075	2.592793
40	6	0	-5.168738	-0.007054	-0.037851
41	6	0	-5.889376	1.128814	-0.446844
42	1	0	-5.360032	2.019451	-0.773094
43	6	0	-7.281249	1.139726	-0.399726
44	1	0	-7.833129	2.021313	-0.703664
45	6	0	-7.974128	0.010151	0.052257
46	6	0	-7.265478	-1.133712	0.442375
47	1	0	-7.825782	-2.004377	0.764526
48	6	0	-5.876896	-1.141170	0.402834

49	1	0	−5.336947	−2.044450	0.672348
50	6	0	−9.464791	−0.030707	0.148511
51	6	0	3.928762	1.165949	0.040405
52	6	0	5.317476	1.206436	0.200040
53	1	0	5.827095	2.156719	0.286197
54	6	0	6.025239	0.012391	0.249781
55	1	0	7.106389	0.014662	0.338285
56	6	0	5.333975	−1.188698	0.180866
57	1	0	5.879181	−2.121189	0.181121
58	6	0	3.933852	−1.175282	0.098919
59	6	0	3.846422	−3.541354	0.849057
60	1	0	3.064196	−4.045844	1.429338
61	1	0	4.577815	−3.161964	1.562261
62	6	0	4.443102	−4.493806	−0.177705
63	1	0	5.203972	−3.978279	−0.773052
64	1	0	4.933577	−5.345675	0.302685
65	6	0	3.302823	−4.989616	−1.067541
66	1	0	3.656917	−5.217779	−2.081249
67	1	0	2.891071	−5.920733	−0.658696
68	6	0	1.014971	−4.618007	−1.858670
69	1	0	0.758691	−5.565044	−1.367681
70	1	0	1.324342	−4.861481	−2.884212
71	6	0	−0.169728	−3.665439	−1.873014
72	1	0	−0.697548	−3.685704	−0.912396
73	1	0	−0.880148	−3.980718	−2.643291
74	6	0	0.349775	−2.256125	−2.135962
75	1	0	0.846898	−2.210734	−3.116516
76	1	0	−0.470758	−1.541264	−2.161438
77	6	0	2.187426	−2.740493	−0.736989
78	6	0	3.868786	3.452899	−0.934407
79	1	0	4.665619	3.005767	−1.531968
80	1	0	3.129155	3.866256	−1.631727
81	6	0	4.385161	4.554774	−0.013281
82	1	0	4.801080	5.379961	−0.599895
83	1	0	5.185811	4.172755	0.625958
84	6	0	3.209640	5.081653	0.816615
85	1	0	2.761846	5.947658	0.313815
86	1	0	3.551348	5.427360	1.800467
87	6	0	0.952877	4.602129	1.735734
88	1	0	0.142627	4.825022	1.026735
89	1	0	1.234832	5.541770	2.216490
90	6	0	0.522002	3.563195	2.760472
91	1	0	1.320395	3.433837	3.500452
92	1	0	−0.371810	3.894455	3.297725
93	6	0	0.240467	2.252205	2.032739
94	1	0	0.179213	1.431864	2.754549
95	1	0	−0.737418	2.309779	1.536443
96	6	0	2.158409	2.778633	0.670162

Table S11. Optimized Atomic coordinates obtained from DFT calculations of [**2**]$^{2+}$

```
---------------------------------------------------------------------
Center     Atomic     Atomic          Coordinates (Angstroms)
Number     Number     Type         X             Y             Z
---------------------------------------------------------------------
   1         44          0       1.119764     -0.055110      0.050209
   2          8          0      -9.815397      0.625450     -1.104262
   3          1          0     -10.612062      0.420588     -1.391600
   4          8          0      -9.953049     -1.347678     -0.054852
   5          7          0       0.651645      1.130166     -1.592385
   6          7          0      -0.822994     -0.094467      0.143465
   7          7          0       0.819835     -1.271151      1.729503
   8          7          0       3.186756      0.080111     -0.017404
   9          7          0       3.358353     -2.276612     -0.066084
  10          7          0       2.326920     -3.819555     -1.500851
  11          7          0       1.339613     -1.728120     -1.141563
  12          7          0       2.967352      2.461860     -0.060684
  13          7          0       1.655652      4.001086      1.113603
  14          7          0       1.158899      1.715005      1.189924
  15          6          0      -0.664243      1.524482     -1.569607
  16          6          0      -1.113523      2.509414     -2.427671
  17          1          0      -2.044565      2.804910     -2.383613
  18          6          0      -0.251577      3.078681     -3.351888
  19          1          0      -0.549874      3.817937     -3.920056
  20          6          0       1.039094      2.584339     -3.456483
  21          1          0       1.644233      2.917945     -4.147602
  22          6          0       1.457625      1.610327     -2.566431
  23          1          0       2.364937      1.255957     -2.641316
  24          6          0      -1.522852      0.774123     -0.636985
  25          6          0      -2.894269      0.838427     -0.542592
  26          1          0      -3.388936      1.474033     -1.095740
  27          6          0      -3.587065      0.000941      0.335627
  28          6          0      -2.838983     -0.852416      1.162916
  29          1          0      -3.289454     -1.426719      1.813413
  30          6          0      -1.449918     -0.874272      1.051871
  31          6          0      -0.511672     -1.593598      1.916683
  32          6          0      -0.893172     -2.488421      2.908694
  33          1          0      -1.832290     -2.745363      3.001963
  34          6          0       0.058302     -3.011499      3.762873
  35          1          0      -0.200623     -3.651389      4.455684
  36          6          0       1.385352     -2.619388      3.629170
  37          1          0       2.067184     -2.937458      4.252876
  38          6          0       1.718494     -1.771810      2.598704
  39          1          0       2.654919     -1.516321      2.487229
  40          6          0      -5.086196     -0.019399      0.329947
  41          6          0      -5.798466      1.045964     -0.227770
  42          1          0      -5.326736      1.868861     -0.467780
  43          6          0      -7.162528      0.958919     -0.445525
  44          1          0      -7.643610      1.710952     -0.844788
  45          6          0      -7.849085     -0.197448     -0.094299
```

46	6	0	−7.170295	−1.217862	0.558311
47	1	0	−7.663824	−1.999115	0.879524
48	6	0	−5.786213	−1.136158	0.760721
49	1	0	−5.315719	−1.868444	1.206254
50	6	0	−9.317291	−0.398446	−0.396752
51	6	0	3.782413	1.306057	0.035785
52	6	0	5.154691	1.441186	0.127880
53	1	0	5.562326	2.327721	0.185446
54	7	0	5.948076	0.325423	0.139063
55	6	0	5.363992	−0.916422	0.026870
56	1	0	5.926211	−1.715687	−0.011503
57	6	0	3.983182	−1.021433	−0.031929
58	6	0	4.117479	−3.445456	0.403539
59	1	0	3.507619	−4.063282	0.919704
60	1	0	4.860667	−3.147148	1.018066
61	6	0	4.693722	−4.170839	−0.796874
62	1	0	5.281056	−3.545670	−1.330704
63	1	0	5.254118	−4.953612	−0.494502
64	6	0	3.535606	−4.655668	−1.648427
65	1	0	3.815506	−4.656759	−2.618431
66	1	0	3.309134	−5.604071	−1.389866
67	6	0	1.148341	−4.400428	−2.147689
68	1	0	0.952770	−5.300198	−1.732450
69	1	0	1.346717	−4.546987	−3.127224
70	6	0	−0.066842	−3.515435	−2.013785
71	1	0	−0.485026	−3.629343	−1.101547
72	1	0	−0.753387	−3.759133	−2.713163
73	6	0	0.389486	−2.079575	−2.202038
74	1	0	0.829594	−1.976186	−3.105265
75	1	0	−0.405796	−1.458757	−2.165090
76	6	0	2.300861	−2.589867	−0.945520
77	6	0	3.527683	3.590478	−0.845588
78	1	0	4.465319	3.353243	−1.135938
79	1	0	2.970780	3.716064	−1.679464
80	6	0	3.559388	4.785231	−0.127357
81	1	0	3.686050	5.538446	−0.788936
82	1	0	4.391381	4.771855	0.451543
83	6	0	2.453131	5.139196	0.722427
84	1	0	1.862306	5.800222	0.238646
85	1	0	2.807443	5.591955	1.552865
86	6	0	0.438646	4.309650	1.857260
87	1	0	−0.353320	4.330761	1.228520
88	1	0	0.523642	5.217929	2.289709
89	6	0	0.229186	3.261028	2.908247
90	1	0	0.988909	3.289153	3.573355
91	1	0	−0.631055	3.439263	3.405256
92	6	0	0.170484	1.912407	2.261551
93	1	0	0.315299	1.206454	2.968684
94	1	0	−0.753989	1.775650	1.878067
95	6	0	1.891927	2.706353	0.780695

References:

1. G. A.Crosby, J. N. Demas, *J. Phys. Chem.*, 1971, **75**, 991.
2. K. Suzuki, A. Kobayashi, S. Kaneko, K. Takehira, T. Yoshihara, H. Ishida, Y. Shiina, S. Oishi, S. Tobita, *Phys. Chem. Chem. Phys.*, 2009, **11**, 9850.
3. A. K. Pal, N. Zaccheroni, S. Campagna, G. S. Hanan, *Chem. Commun.*, 2014, **50**, 6846.
4. A. K. Pal, G. S. Hanan, *Dalton Trans.*, 2014, **43**, 11811.
5. J. Wang, G. S. Hanan, *Synlett*, 2005, **8**, 1251.
6. *APEX2 (2013); Bruker Molecular Analysis Research Tool.* Bruker AXS Inc., Madison, WI 53719-1173.
7. (a) SAINT (2013) V8.34A; Integration Software for Single Crystal Data. Bruker AXS Inc., Madison, WI 53719-1173. (b) SAINT (2013) V8.34A; Integration Software for Single Crystal Data. Bruker AXS Inc., Madison, WI 53719-1173.
8. Sheldrick, G. M. (1996). *SADABS*, Bruker Area Detector Absorption Corrections. Bruker AXS Inc., Madison, WI 53719-1173.
9. *SHELXTL (2012) version 6.14*; Bruker Analytical X-ray Systems Inc., Madison, WI 53719-1173.
10. M. J. Frisch, G. W. Trucks, H. B. Schlegel, G. E. Scuseria, M. A. Robb, J. R. Cheeseman, J. A. Montgomery, T. J. Vreven, K. N. Kudin, J. C. Burant, J. M. S. Millam, J. Tomasi, V. Barone, B. Mennucci, M. Cossi, G. Scalmani, N. Rega, G. A. Petersson, H. Nakatsuji, M. Hada, M. Ehara, K. Toyota, R. Fukuda, J. Hasegawa, M. Ishida, T. Nakajima, Y. Honda, O. Kitao, H. Nakai, M. Klene, X. Li, J. E. Knox, H. P. Hratchian, J. B. Cross, C. Adamo, J. Jaramillo, R. Gomperts, R. E. Startmann, O. Yazyev, A. J. Austin, R. Cammi, C. Pomelli, J. W. Ochterski, P. Y.Ayala, K. Morokuma, G. A. Voth, P. Salvador, J. J. Dannenberg, V. G. Zakrzewski, J. M. Dapprich, A. D. Daniels, M. C. Strain, O. Farkas, D. K. Malick, A. D. Rabuck, K. Raghavachari, J. B. Foresman, J. V. Ortiz, Q. Cui, A. G. Baboul, S. Cliffors, J. B. Cioslowski, G. Liu, A. Liashenko, I. Piskorz, L. M. R. Komaromi, D. J. Fox, T. Keith, M. A. Al–Laham, C. Y. Peng, A. Manayakkara, M. Challacombe, P. M. W. Gill, B. G. Johnson, W. Chen, M. W. Wong, C. Gonzalez, J. A. Pople, Gaussian 2009, Revision D.01; Gaussian, Inc., Wallingford CT, 2013.
11. A. D. Becke, *J. Chem. Phys.*, 1993, **98**, 5648.
12. C. Lee, W. Yang, R. G. Parr, *Phys. Rev. B: Condens. Matter* 1988, **37**, 785.
13. A. D. McLean, G. S. Chandler, *J. Chem. Phys.*, 1980, **72**, 5639.
14. P. J. Hay, W. R. Wadt, *J. Chem. Phys.*, 1985, **82**, 270.
15. (a) M. E. Casida, C. Jamorski, K. C. Casida, D. R. Salahub, *J. Chem. Phys.*, 1998, **108**, 4439. (b) R. E. Stratmann, G. E. Scuseria, M. J. Frisch, *J. Chem. Phys.*, 1998, **109**, 8218.
16. (a) M. Cossi, N. Rega, G. Scalmani, V. Barone, *J. Comput. Chem.*, 2003, **24**, 669. (b) M. Cossi, V. Barone, *J. Chem. Phys.* 2001, **115**, 4708. (c) V. Barone, M. Cossi, *J. Phys. Chem. A*, 1998, **102**, 1995.
17. W. R. Browne, N. M. O'Boyle, J. J. McGarvey, J. G. Vos, *Chem. Soc. Rev.*, 2005, **34**, 641.
18. D. A. Zhurko, G. A. Zhurko, *ChemCraft 1.5*; Plimus: San Diego, CA. Available at http://www.chemcraftprog.com.
19. M. Maestri, N. Armaroli, V. Balzani, E. C. Constable, A. M. W. C. Thompson, *Inorg. Chem.*, 1995, **34**, 2759.